Can Short- and Middle-Range Hybrids Describe the Hyperpolarizabilities of Long-Range Charge-Transfer Compounds?

ARTICLE *in* THE JOURNAL OF PHYSICAL CHEMISTRY A · NOVEMBER 2014

Impact Factor: 2.69 · DOI: 10.1021/jp510062b

4 AUTHORS, INCLUDING:

Nuha Wazzan
King Abdulaziz University
17 PUBLICATIONS **59** CITATIONS
SEE PROFILE

Abdullah M. Asiri
King Abdulaziz University
1,155 PUBLICATIONS **6,804** CITATIONS
SEE PROFILE

THE JOURNAL OF PHYSICAL CHEMISTRY A

Article

pubs.acs.org/JPCA

Can Short- and Middle-Range Hybrids Describe the Hyperpolarizabilities of Long-Range Charge-Transfer Compounds?

Alejandro J. Garza,[†] Nuha A. Wazzan,[‡] Abdullah M. Asiri,[‡,§] and Gustavo E. Scuseria*[,†,‡,∥]

[†]Department of Chemistry and [∥]Department of Physics and Astronomy, Rice University, Houston, Texas 77251-1892, United States
[‡]Chemistry Department, Faculty of Science and [§]Center of Excellence for Advanced Materials Research (CEAMR), King Abdulaziz University, Jeddah 21589, Saudi Arabia

ABSTRACT: The hyperpolarizabilities of five prototypical and four recently synthesized long-range charge-transfer (CT) organic compounds are calculated using short- and middle-range (SR and MR) hybrid functionals. These results are compared with data from MP2 and other DFT methods including GGAs, global hybrids, long-range corrected functionals (LC-DFT), and optimally tuned LC-DFT. Although it is commonly believed that the overestimation of hyperpolarizabilities associated with CT excitations by GGA and global hybrid functionals is the result of their wrong asymptotic exchange potential, and that LC-DFT heals this issue, we show here that SR and MR functionals yield results similar to those from LC-DFT. Hence, the long-range correction *per se* does not appear to be the key element in the well-known improved description of hyperpolarizabilities by LC-DFT. Rather, we argue that the inclusion of substantial amounts of Hartree−Fock exchange, which reduces the many-electron self-interaction error, is responsible for the relatively good results afforded by range separated hybrids. Additionally, we evaluate the effects of solvent and frequency on hyperpolarizabilities computed by SR and MR hybrids and compare these predictions with other DFT methods and available experimental data.

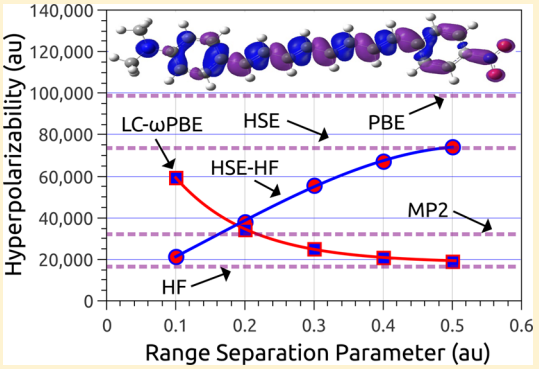

INTRODUCTION

Consider a long-range charge-transfer (CT) excitation between donor and acceptor groups separated by a distance R. Assuming a substantial degree of CT, the transition energy E_{CT} (in au) is approximately[1,2]

$$E_{CT} \approx IP^{D} - EA^{A} - 1/R \tag{1}$$

where IP^{D} is the ionization potential of the donor, EA^{A} is the electron affinity of the acceptor, and $1/R$ is the interaction between them. The energy E_{CT} is related to the hyperpolarizability of the CT species; this is most easily seen in the two-state model for the first-order (static) hyperpolarizability[3,4]

$$\beta_z^{T} = \frac{6\mu_{eg,z}^{2}(\mu_{e,z} - \mu_{g,z})}{E_{CT}^{2}} \tag{2}$$

where $\mu_{eg,z} = \langle \Psi_e | \hat{\mu}_z | \Psi_g \rangle$, $\mu_{e,z}$ and $\mu_{g,z}$ are transition and dipole moments for the excited and ground states in the z direction. Although eq 2 does not yield quantitative results (it overestimates β_z^{T} by a factor of about 2), it usually reproduces qualitative trends correctly and accounts for a large part of the hyperpolarizability in a converged sum-over-states expression.[5−7] Thus, because of their typically low IP^{D} and EA^{A}, small $1/R$, and large dipole moments, materials such as donor−acceptor organic compounds with long-range CT often display large β_z^{T} values.[8−11] This has generated much interest around this kind of compound owing to the applications of materials with large hyperpolarizabilities in nonlinear optics[12−19] (NLO), and a considerable amount of effort in this area of research has been devoted to the theoretical prediction of NLO properties via computational methods of quantum chemistry.[19−28]

It was recognized early on that the theoretical determination of hyperpolarizabilities was very challenging for *ab initio* and semiempirical methods.[8,12,20] The advent of modern density functional theory (DFT) methods, very successful in many areas across chemistry and materials science, does not solve this problem. In fact, the description of CT excitations by time-dependent (TD)DFT using popular global hybrids and generalized gradient approximations (GGAs) is fundamentally flawed, often leading to gross underestimations of E_{CT} and, consequently, exaggeration of β_z^{T}.[23−25] In TDDFT, the approximate expression for E_{CT} comparable to eq 1 yields[1,2]

$$E_{CT}^{TDDFT} \approx \epsilon_a^{A} - \epsilon_i^{D} + [ai|f_{xc}|ia] \tag{3}$$

where ϵ_i^{D} is the energy of an occupied orbital φ_i localized in the donor, ϵ_a^{A} is the energy of an unoccupied orbital φ_a in the acceptor, f_{xc} is the exchange−correlation kernel, and $[ai|f_{xc}|ia] = \int \varphi_a^{*}(r_1)\,\varphi_i^{*}(r_2)\,f_{xc}(r_1,r_2)\,\varphi_i(r_1)\,\varphi_a(r_2)\,dr_1\,dr_2$. In commonly used functionals, the $\epsilon_a^{A} - \epsilon_i^{D}$ term does not approximate $IP^{D} - EA^{A}$. Additionally, in long-range CT excitations, $[ai|f_{xc}|ia]$

Received: October 5, 2014
Revised: November 25, 2014
Published: November 26, 2014

   dx.doi.org/10.1021/jp510062b | J. Phys. Chem. A 2014, 118, 11787−11796

decays exponentially (for GGAs) yielding asymptotically zero or c/R (for hybrids with $c < 1$) rather than $1/R$.[1,2] Although hybrids with 100% Hartree−Fock (HF) exchange (HF has the correct asymptotic behavior) should in principle solve this issue, these approaches are seldom satisfactory due to the reliance of DFT on error cancellation between inexact exchange and correlation terms. Thus, the poor CT excitation energies afforded by TDDFT are often blamed on these two fundamental deficiencies.

Methods within TDDFT have been developed that overcome the above-mentioned problems. The $1/R$ term can be recovered by separating the Coulomb operator into complementary short- and long-range parts, and evaluating the exchange energy in the long-range with pure HF exchange. This is the idea behind long-range corrected (LC)-DFT functionals,[29−34] which have been shown to provide an improved description of long-range properties (including CT excitations and hyperpolarizabilities) as compared to that by global hybrids and GGAs.[35−48] Furthermore, the range-separation parameter of LC-DFT can be optimized *ab initio* for the system of interest by demanding that the molecule, and its corresponding anion, obey Koopman's theorem,[49] so that $\epsilon_a^A - \epsilon_i^D$ approximates $IP^D - EA^A$.[50−53] This methodology, often referred to as gap tuning or optimally tuned LC-DFT, further improves the accuracy in predictions of CT energies and first-order hyperpolarizabilities[50−56] (if the system is not very large,[55,56] because the tuning procedure is not size extensive). A recent review on tuned LC-DFT is available in ref 57. Here we also note that there are functionals analogous to LC-DFT but that evaluate HF exchange only in the short-range (SR) or middle-range (MR; the Coulomb operator is divided in three parts). However, these functionals are rarely used in hyperpolarizability calculations because it is believed that the incorrect asymptotic behavior of the exchange potential would lead to the problems that appear in GGAs.

In this paper, we use SR and MR hybrid functionals to calculate the hyperpolarizabilities of five prototypical CT donor−acceptor chromophores [*p*-nitroaniline (PNA), (dimethylamino)nitrostilbene (DANS), and three DANS derivatives with extended π-conjugated bridges, (DANS*n*)] as well as four recently synthesized[58−61] potential NLO compounds (2,3-dihydro-1*H*-inden-1-one derivatives **1**−**4**). The structures of these molecules are shown in Figure 1. The hyperpolarizabilities predicted by SR and MR hybrids are compared with results from MP2 calculations and other DFT methods including GGAs, global hybrids, LC-DFT, and tuned LC-DFT. It is shown that SR and MR hybrids can yield results comparable to those from LC-DFT, suggesting that the long-range correction (and the associated $1/R$ asymptotic exchange potential) *per se* is not the key element in the improved description of CT processes by LC-DFT. Rather, following previous studies by Henderson et al.,[62] we argue that the inclusion of substantial amounts of HF exchange, which reduces the many-electron self-interaction error (SIE), is responsible for the relatively good results afforded by range-separated hybrids. We must also mention here that Tozer[63] provided an explanation for the failure of TDDFT in describing long-range CT excitations based on the lack of an integer discontinuity in local functionals. Our results here support the theories in refs 62 and 63 and suggest that SR and MR hybrids may too be useful for the prediction of hyperpolarizabilities in long-range CT organic compounds. In addition, we evaluate the effects of solvent and frequency on the hyperpolarizabilities computed by these functionals, comparing results with data from experiment and other DFT methods.

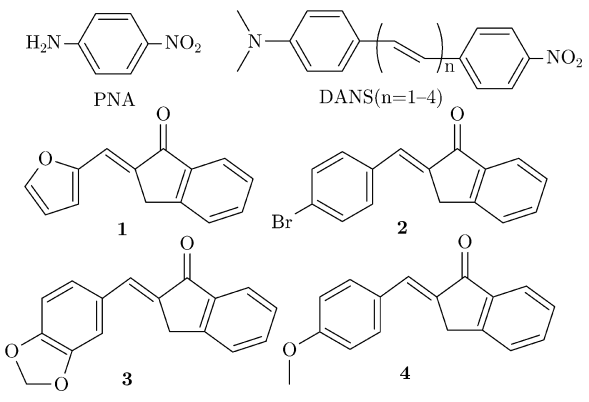

Figure 1. Molecular structures of the compounds studied in this work.

THEORY AND METHODS

Range-Separated Hybrids (RSHs) and Optimal Tuning. Here we give a brief overview of RSHs and describe the functionals employed in this work. As mentioned in the Introduction, range separation is accomplished by dividing the (interelectronic) Coulomb operator into complementary parts. For a three-range hybrid we have

$$\frac{1}{r_{12}} = \frac{\mathcal{F}_{SR}(r_{12})}{r_{12}} + \frac{\mathcal{F}_{MR}(r_{12})}{r_{12}} + \frac{\mathcal{F}_{LR}(r_{12})}{r_{12}} \quad (4)$$

For all RSHs utilized here, the range-separation functions are defined in terms of the standard error function erf(x) so that $\mathcal{F}_{SR} = 1 - \mathrm{erf}(\omega_{SR} r_{12})$, $\mathcal{F}_{LR} = \mathrm{erf}(\omega_{LR} r_{12})$, and $\mathcal{F}_{MR} = \mathrm{erf}(\omega_{SR} r_{12}) - \mathrm{erf}(\omega_{LR} r_{12})$. The ω parameters define the range separation and $\omega_{LR} \leq \omega_{SR}$; for LC-DFT and SR hybrids $\omega_{SR} = \omega_{LR} = \omega$ (i.e., $\mathcal{F}_{MR} = 0$). The exchange energy E_x for any hybrid or RSH (up to three-range) can now be written as

$$E_x = (1 - c_{SR})E_x^{SR-DFT} + c_{SR}E_x^{SR-HF} + (1 - c_{MR})E_x^{MR-DFT} + c_{MR}E_x^{MR-HF} + (1 - c_{LR})E_x^{LR-DFT} + c_{LR}E_x^{LR-HF} \quad (5)$$

For convenience, the parameters in eq 5 for all the functionals for which we present data are listed in Table 1.

Table 1. Parameters in Eq 5 for All Functionals Utilized in This Work (All ω Values in au)

functional	ω_{SR}	ω_{LR}	c_{SR}	c_{MR}	c_{LR}
PBE	0	0	0	0	0
PBE0	0	0	0.25	0	0
B3LYP	0	0	0.2	0	0
M06-HF	0	0	1	0	0
LC-PBE	0.3	0.3	0	0	1
LC-ωPBE	0.4	0.4	0	0	1
ωB97X-D	0.2	0.2	0.222036	0	1
CAM-B3LYP	0.33	0.33	0.19	0	0.65
HSE	0.11	0.11	0.25	0	0
HISS	0.84	0.2	0	0.6	0
HSE-HF	0.1	0.1	1	0	0
HISS-HF	0.84	0.2	0	1	0

dx.doi.org/10.1021/jp510062b | J. Phys. Chem. A 2014, 118, 11787−11796

These parameters correspond to those recommended in the literature (see also the Computational Details) except for the functionals by Heyd et al.[64] (HSE = HSE06; see also ref 62 and Henderson et al.[65,66] (HISS). The reason for this is that HSE and HISS commonly use $c_{SR} = 0.25$ and $c_{MR} = 0.6$, respectively, but these fractions of HF exchange are too low for typical gas-phase hyperpolarizability calculations. Thus, we made these values both equal to 1 so that the magnitude of HF exchange in these functionals could be comparable to that of LC-DFT methods. We denote these versions of HSE and HISS as HSE-HF and HISS-HF, to emphasize the use 100% HF exchange in the short and middle ranges, respectively, and to distinguish them from their default counterparts.

Additionally, the ω value for HSE-HF was determined by optimal tuning[50−53] using the methodology described in ref 55; the optimal value for all molecules (in gas phase) studied here was $\omega = 0.1$ au. We note, however, that this value is very close to the standard $\omega = 0.11$ au of HSE. For completeness, we outline the aforementioned tuning procedure as follows: the parameter ω is chosen as the minimizer of the function

$$J_{\text{gap}}(\omega) = \sum_{i=0}^{1} |\epsilon_{\text{H}}^{\omega}(N+i) + \text{IP}^{\omega}(N+i)| \tag{6}$$

where $\epsilon_{\text{H}}^{\omega}(N)$ is the energy of the HOMO and $\text{IP}^{\omega}(N)$ the ionization potential for the N-electron system. That is, ω is a free variable to optimize to enforce Koopman's theorem, which holds for the exact functional,[67] on the system of interest and its corresponding anion. As in ref 55, we take a minimalist approach and select the ω value that minimizes J_{gap} among the set $\omega/\text{au} = \{1 \times 10^{-4}, 0.1, 0.2, 0.3, 0.4, 0.5\}$. This optimal tuning methodology has already been shown to be quite appropriate for the calculation of properties of long-range CT compounds with LC-DFT[6,55] and is also applied here to some of the LC-DFT functionals in Table 1 and to HSE-HF in polar media. Thus, from now on, we shall use an asterisk (*) to distinguish between tuned and nontuned LC-DFT methods, e.g., LC-ωPBE* is the optimally tuned version of LC-ωPBE.

Hyperpolarizabilities. To avoid any confusion caused by the various conventions for hyperpolarizabilities available,[4,68] we clarify in this section the conventions and hyperpolarizability measures employed here. All hyperpolarizabilities in this work are reported in the "T" convention, which defines (hyper)polarizabilities based on the Taylor expansion of the induced dipole moment $\boldsymbol{\mu}$ as a function of the field $\mathbf{F}$

$$\mu_i(\mathbf{F}) = \mu_i^0 + \alpha_{ij}F_j + \frac{1}{2!}\beta_{ijk}F_jF_k + \frac{1}{3!}\gamma_{ijkl}F_jF_kF_l + \cdots \tag{7}$$

where $\boldsymbol{\mu}^0$ is the dipole moment in the absence of the field, $\boldsymbol{\alpha}$ is the polarizability, $\boldsymbol{\beta}$ is the first-order hyperpolarizability, $\boldsymbol{\gamma}$ is the second-order hyperpolarizability, and so on. The actual hyperpolarizability measure used here is $\beta_{\parallel}$, which is given by

$$\beta_{\parallel} = \frac{1}{5}\sum_{i=x,y,z}(\beta_{zii} + \beta_{izi} + \beta_{iiz}) \tag{8}$$

where the z axis is aligned with the dipole moment of the molecule. We note that $\beta_{\parallel} = (3/5)\beta_z^{\text{T}}$. Additionally, in some calculations, we also provide the total hyperpolarizability β_{tot} defined as

$$\beta_{\text{tot}} = \sqrt{\beta_x^2 + \beta_y^2 + \beta_z^2} \tag{9}$$

where

$$\beta_i = \beta_{iii} + \frac{1}{3}\sum_{i\neq j}(\beta_{ijj} + \beta_{jij} + \beta_{jji}) \tag{10}$$

The β_{tot} values given here are frequency-independent and the coordinate system is defined by the standard orientation of the molecules. This is purely a convenience based on the way hyperpolarizability tensors are printed in the output file generated by the program used for the calculations (see the Computational Details). All hyperpolarizabilities are given in au, which are related to electrostatic units (esu) via the relation 1 au = 8.6393×10^{-33} esu for β_{ijk}. For details regarding the relationship between different hyperpolarizability conventions, the reader is referred to the paper by Reis.[4]

Computational Details. All calculations were carried out using the Gaussian 09 suite of programs[69] which was customized to compute hyperpolarizabilities using the LC-ωPBE functional. Unless otherwise indicated, default parameters were used in all calculations. The internal options (IOps) of the Gaussian software were utilized to set the ω values and HF exchange fractions that differed from their default setup in LC-ωPBE*, HSE-HF, and HISS-HF; HSE and HSE-HF calculations both use the HSEH1PBE keyword. The methods and basis sets used are indicated where appropriate; in general, the 6-31+G(d) or larger basis sets are employed, all of which have been shown to be adequate for the prediction of first-order NLO properties.[70] The geometries of the PNA and DANS*n* molecules were optimized exactly as in ref 54 [B3LYP/6-311G(d,p) level] to enable comparison with some of the results there. Likewise, certain calculations on PNA use the CAM-B3LYP/6-31G(d,p) geometries of ref 55 to allow for comparisons too. For **1**−**4**, CAM-B3LYP/6-31+G(d,p) geometries were utilized because this method provided good agreement with available crystal structures.[58−61] Excited state calculations were done with TDDFT. All computations reported to be done in solvent utilized the polarizable continuum model[71] (PCM) in the nonequilibrium solvation limit.

RESULTS AND DISCUSSION

The reasoning for which we argue that the long-range correction is not the key element in the description of molecular hyperpolarizabilities is as follows: if the asymptotic $1/R$ behavior of the exchange potential is critical to describe $\beta_{\parallel}$, then removing HF exchange from the long range to introduce local exchange instead should lead to a substantial degradation of $\beta_{\parallel}$. As shown here for the prototypical long-range CT compounds PNA and DANS*n*, as well as for **1**−**4**, this does not happen to be the case. Hence, the long-range correction is not essential in the description of molecular hyperpolarizabilities.

PNA and DANSn. The static $\beta_{\parallel}$ values for the PNA and DANS*n* molecules predicted by different methods are summarized in Table 2 (selected data from refs 54 and 72 are included for comparison); Figure 2 displays the trends in these data and the ratios $\beta_{\parallel}/\beta_{\parallel}^{\text{PNA}}$ with increasing donor−acceptor distance. It is readily appreciated that the results of HSE and HSE-HF are similar to those of PBE0 and M06-HF, respectively. That is, hybrids having a certain fraction of HF exchange only in the SR yield hyperpolarizabilities comparable to those of global hybrids having the same fraction of HF exchange. Moreover, the HSE-HF and LC-ωPBE $\beta_{\parallel}$ values are also very close to each other, especially for the DANS*n* chromophores for which the differences in $\beta_{\parallel}$ are just about 5%. Likewise, the HISS-HF and LC-PBE* hyperpolarizabilities are

Table 2. Static $\beta_{\parallel}$ Values (au) Calculated by Different Methods Using the 6-31+G(d) Basis[a]

method	PNA	DANS	DANS2	DANS3	DANS4
CCSD	1066				
MP2	1085	9691	16891	23204	32061
HF	581	5191	8298	11943	16443
PBE	1056	23565	40611	64618	98731
PBE0	980	15572	26746	41757	61789
HSE	979	17492	30080	48043	73532
HSE-HF	574	6270	10160	15192	21364
M06-HF	667	6402	10163	14858	20334
LC-ωPBE	755	6684	10593	15418	21031
LC-PBE	863	8380	13004	19030	26499
LC-PBE*	872	10243	16747	26592	39673
HISS-HF	792	11145	18826	29312	43277

[a]The CCSD value is from ref 72; MP2, HF, PBE, PBE0, LC-PBE and LC-PBE* data are from ref 54.

within a range of ca. 10% of each other. These differences are rather negligible considering the wide range of $\beta_{\parallel}$ values afforded by the methods in Table 2, e.g., up to ~500% difference between HF and PBE.

Looking at the right panel of Figure 2, one can notice a larger difference with respect to MP2 (which, though not perfect, is reasonably accurate[24,42,70,73]) in the $\beta_{\parallel}/\beta_{\parallel}^{\mathrm{PNA}}$ ratios of HSE-HF as compared to those of HF, M06-HF LC-PBE, and LC-ωPBE. However, this better agreement with MP2 for the latter methods cannot be attributed solely to the right asymptotic exchange potential; LC-PBE* differs even more from MP2 than HSE-HF. Instead, the larger $\beta_{\parallel}/\beta_{\parallel}^{\mathrm{PNA}}$ ratios predicted by HSE-HF, LC-PBE*, and HISS-HF can be attributed to the incorporation of lower amounts of HF exchange with increasing molecular size (for LC-PBE*, the optimal ω decreases with molecular length[54]). Thus, among the hyperpolarizability data given by M06-HF, LC-ωPBE, and HSE-HF (hybrids with 100% HF exchange in the full, long, and short range, respectively), no significant difference is found that can be related to the asymptotic exchange potential.

The above observations are in agreement with the results by Henderson et al.,[62] who found HSE to be of similar quality to PBE0 for long-range properties such as Rydberg excitations, polarizabilities of H_2 chains, and even the vibrational spectra of a periodic H_2O chain. By analyzing the dissociation curves for H_2^+, He_2^+, and Ar_2^+, the authors in ref 62 concluded that the many-electron SIEs (also known as delocalization error) were very similar for HSE and PBE0. The many-electron SIE has been related to the deviation from linearity of the energy when the electron number is changed between adjacent integers—a constraint the exact functional must satisfy.[67] On this basis, Vydrov et al.[74] have shown that LC-DFT drastically reduces the many-electron SIE of GGAs and commonly used global hybrids. In addition, for PNA and DANS, Sun and Autschbach[54] showed that LC-DFT and tuned LC-DFT both yield a nearly perfect linear dependence for the energy as a function of fractional electron number between adjacent integers. Considering all this and the results here, it seems more plausible to associate the improved description of hyperpolarizabilities by LC-DFT with the reduction of many-electron SIE, rather than the correct asymptotic exchange potential, and to conclude that SR and MR hybrids can yield results comparable to those of global hybrids or LC-DFT (depending on the specific formulations of the functionals).

Having said this, we must note two things. The first one is that even the failure of semilocal functionals to approximate the ideal CT excitation energy $E_{\mathrm{CT}} \approx \mathrm{IP}^{\mathrm{D}} - \mathrm{EA}^{\mathrm{A}} - 1/R$ (eq 1) by $E_{\mathrm{CT}}^{\mathrm{TDDFT}} \approx \epsilon_a^{\mathrm{A}} - \epsilon_i^{\mathrm{D}} + [ai|f_{\mathrm{xc}}|ia]$ (eq 3) can be understood as a self-interaction error.[75] Basically, the TDDFT expression for $\epsilon_a^{\mathrm{A}} - \epsilon_i^{\mathrm{D}}$ contains the Coulomb term between orbitals a and i, i.e., the integral $(aa|ii)$. However, orbital i is empty in the CT state, meaning that the excited electron in orbital a interacts with itself in orbital i. Inclusion of HF exchange cancels out the $(aa|ii)$ contribution, reducing the self-interaction and recovering the $1/R$ term. The other thing to note is that Tozer[63] has also provided an explanation for the failure of TDDFT in describing long-range CT excitations based on the lack of an integer discontinuity in approximate functionals: the exact exchange–correlation potential is discontinuous at integer numbers of electrons.[67] Moreover, Tozer's theory has predictive power and estimates the TDDFT error in a CT excitation as

$$E_{\mathrm{CT}}^{\mathrm{TDDFT}} - E_{\mathrm{CT}}^{\mathrm{Exact}} \approx -(\epsilon_{\mathrm{H}}^{\mathrm{A}} + \mathrm{IP}^{\mathrm{A}}) - (\epsilon_{\mathrm{H}}^{\mathrm{D}} + \mathrm{IP}^{\mathrm{D}}) \qquad (11)$$

where IP^{D} and IP^{A} are exact ionization potentials for the donor and acceptor, respectively, whereas the orbital energies are from the density functional. If, for a molecular system, we approximate $\epsilon_{\mathrm{H}}^{\mathrm{A}} \approx \epsilon_{\mathrm{H}}(N)$, $\epsilon_{\mathrm{H}}^{\mathrm{D}} \approx \epsilon_{\mathrm{H}}(N+1)$, $\mathrm{IP}^{\mathrm{A}} \approx \mathrm{IP}(N)$, and $\mathrm{IP}^{\mathrm{D}} \approx \mathrm{IP}(N+1)$, we see that minimizing J_{gap} in eq 6 also makes the error in eq 11 approach 0. Table 3 shows the E_{CT}

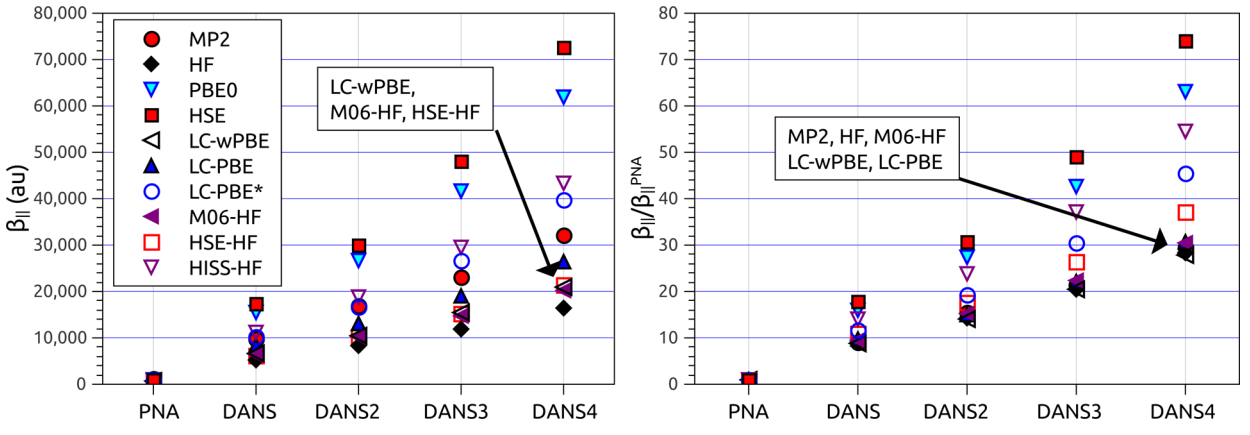

Figure 2. Static $\beta_{\parallel}$ values (left) and $\beta_{\parallel}/\beta_{\parallel}^{\mathrm{PNA}}$ ratios (right) calculated by different methods using the 6-31+G(d) basis. The MP2, HF, PBE0, LC-PBE, and LC-PBE* data were taken from ref 54.

dx.doi.org/10.1021/jp510062b | J. Phys. Chem. A 2014, 118, 11787–11796

Table 3. Charge-Transfer Excitation Energies E_{CT}, Oscillator Strengths f, HOMO Energies for Neutral Species $\epsilon_H(N)$ and Anion $\epsilon_H(N+1)$, J_{gap} and Errors Estimated by Eq 11 for PNA[a]

method	E_{CT}	f	$\epsilon_H(N)$	$\epsilon_H(N+1)$	J_{gap}	eq 11 error	exptl error
exptl	4.28						
EOM-CCSD	4.66	0.45					0.38
PBE	3.52	0.27	−5.76	2.04	5.02	−5.80	−0.76
PBE0	4.08	0.35	−6.77	1.33	3.49	−4.06	−0.20
HSE	4.02	0.34	−6.39	1.68	4.22	−4.80	−0.26
HSE-HF	5.13	0.40	−8.56	−1.16	0.21	0.21	0.85
LC-ωPBE	4.71	0.41	−9.14	−0.92	0.87	0.54	0.43
LC-ωPBE*	4.49	0.39	−8.72	−0.48	0.20	−0.31	0.21
M06-HF	4.88	0.45	−9.58	−1.52	1.34	1.60	0.60
HISS	4.28	0.38	−6.73	2.66	3.75	−5.43	0.00
HISS-HF	4.71	0.42	−7.42	2.08	2.58	−4.17	0.43

[a]All calculations use the 6-31+G(d) basis; energies are in eV, and f, in au. The experimental and EOM-CCSD values are from refs 68 and 78, respectively.

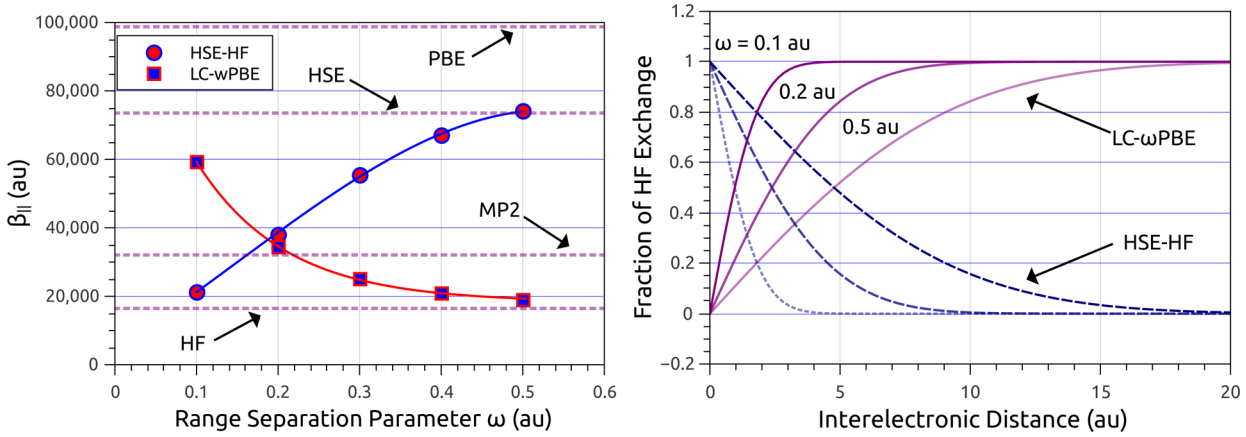

Figure 3. Dependence of $\beta_{||}$ on ω for DANS4 (left) and fraction of HF exchange as a function of r at various ω values (right) for LC-ωPBE and HSE-HF. The $\beta_{||}$ values for DANS4 using HSE-HF with ω = 1.0 and 2.0 au are 88 909 and 95 698 au, respectively.

Table 4. Comparison of Experimental and Theoretical $\beta_{||}$ Data (au) for PNA in Different Media and at Various Wavelengths (nm)[a]

media	λ	exptl	HSE-HF	LC-ωPBE	LC-ωPBE*	HISS	HISS-HF	HSE-HF*	HSE	B3LYP
gas	1064	1072	927	1090	1222	1466	1139	927	1640	1744
1,4-dioxane	inf	2250	1223	1343	1844	1703	1436	1232	1783	1840
1,4-dioxane	1064	2760	1786	2032	3834	2859	2160	1770	3250	3472
1,4-dioxane	1907	1596	1324	1471	2165	1906	1567	1329	2031	2112
acetone	inf	3305	2478	2606	3723	3393	2816	3117	3568	3718
acetone	1064	4317	2317	2461	4438	3429	2631	3030	3833	4109
acetone	1907	2162	1666	1742	2390	2208	1861	1995	2304	2392
methanol	inf	4027	2581	2704	3980	3528	2925	3241	3711	3870
methanol	1064	5334	2302	2434	4772	3379	2600	2983	3767	4035
ME (au)			−1135	−993	172	−328	−854	−800	−104	52
MAE (au)			1135	997	397	536	869	800	526	513
ME (%)			−33	−27	9	5	−22	−24	5	10
MAE (%)			33	27	16	18	24	24	20	22

[a]All calculations use the 6-311+G(d,p) basis. The original experimental values are from various references,[84−88] but have been conveniently compiled and corrected/adapted from different conventions in refs 4 and 89. The geometries [CAM-B3LYP/6-31G(d,p)] and LC-ωPBE, LC-ωPBE*, and B3LYP data are from ref 55. Infinite wavelength corresponds to the static limit.

values of PNA calculated by different methods. J_{gap} and the error estimated by eq 11, using the experimental[76,77] IP = 8.60 eV and EA = 0.91 eV, are also listed there and compared with the error with respect to experiment.[68] Values from high level EOM-CCSD calculations[78] are also given as reference. In general, there is correlation between the error by eq 11 and the actual error, although the agreement is not quantitative. This is similar to previous findings[63] in more extreme cases where the LDA/GGA error is of several electronvolts. However, it is seen that the largest discrepancies between eq 11 and the error occur when $\epsilon_H(N+1)$ is positive, which is a manifestation of severe self-interaction error.[74,79] So, overall, the results here indicate

dx.doi.org/10.1021/jp510062b | J. Phys. Chem. A 2014, 118, 11787−11796

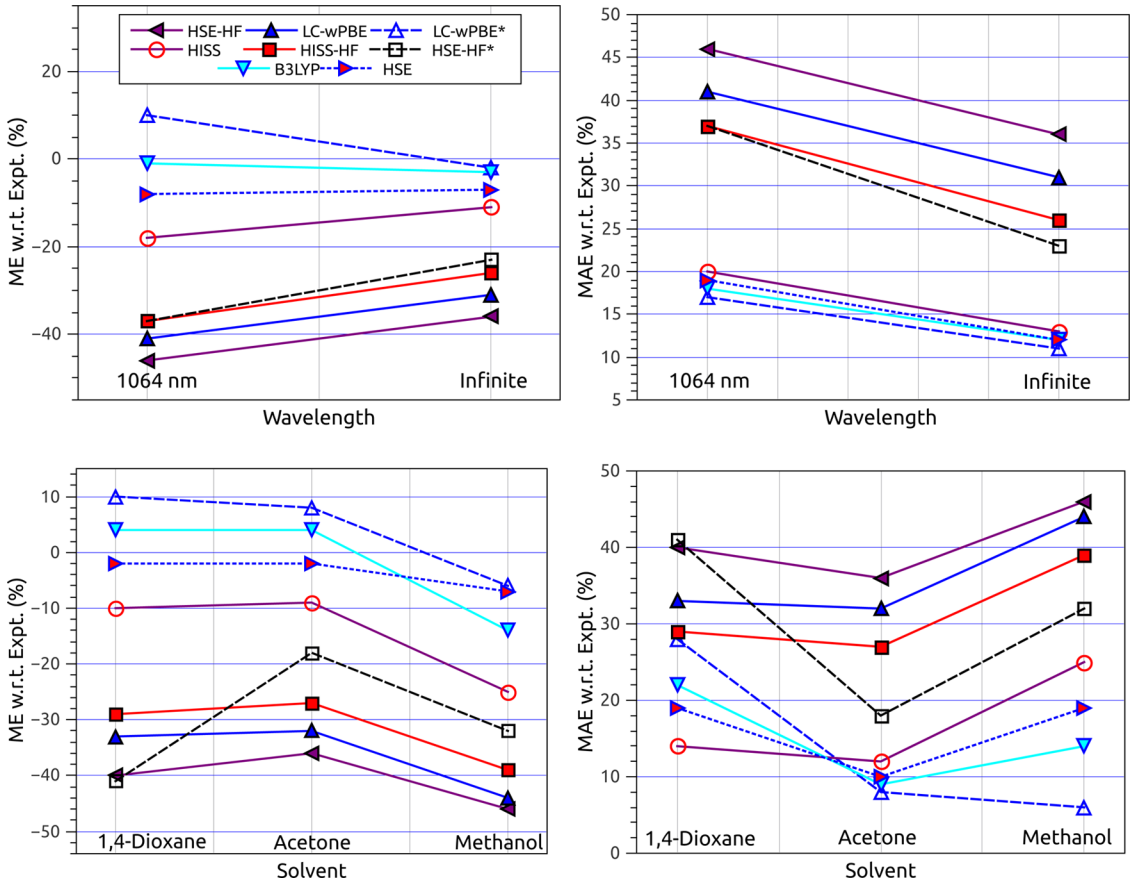

Figure 4. Average errors for the DFT $\beta_{\parallel}$ data of PNA at 1064 nm and infinite wavelength (static limit) in 1,4-dioxane, acetone, and methanol (calculated from the data in Table 4). ME is the mean error (theory − experiment) and MAE the mean absolute error.

that it is indeed more likely to relate better hyperpolarizabilities and CT excitations with reduced SIE due to inclusion of significant fractions of HF exchange along the molecule, and a smaller integer discontinuity error, rather than the shape of the exchange potential. We also note that various works[80−82] have shown that the reduction of the SIE via incorporation of large fractions (~0.75) of HF exchange improves closely related properties, such as orbital energy gaps. However, one should exercise caution when using increased amounts of nonlocal exchange for other types of calculations, as other properties (e.g., thermodynamical) may deteriorate (for an interesting discussion, see ref 83).

Lastly, we point out that it should not be surprising that SR and MR hybrids can produce $\beta_{\parallel}$ values comparable to those of LC-DFT. This is because all these functionals are capable of interpolating between pure local and pure nonlocal (HF) exchange. Because GGAs tend to overestimate hyperpolarizabilities, whereas functionals with 100% HF exchange tend toward the opposite, it follows that all types of RSHs should be capable of providing similar hyperpolarizabilities given the right set of range-separation parameters. This is illustrated in the left panel of Figure 3, which shows the dependence of $\beta_{\parallel}$(DANS4) on ω for HSE-HF and LC-ωPBE; these two methods yield very similar (and close to MP2) $\beta_{\parallel}$ near ω = 0.2 au. The right panel of Figure 3 plots a fraction of HF exchange as a function of interelectronic distance r at various ω values; here it is seen that the fraction of HF exchange in HSE-HF with ω = 0.1 decays to zero only at $r \approx 20$ au, a rather large value, which explains the underestimation of $\beta_{\parallel}$ for PNA. Nevertheless, the donor−acceptor distance for DANS4 is about 36.83 au and even at ω = 0.5 au the $\beta_{\parallel}$ of HSE-HF is still well below PBE. Hence, the long-range exchange does not appear to be of particular importance (compared to the exchange in other ranges) for hyperpolarizability calculations.

Solvent and Frequency Effects. In a recent paper,[55] we evaluated the effects of solvent, frequency, and tuning on the LC-DFT hyperpolarizabilities of PNA. Here, we extend that work to SR and MR hybrids; these results also reinforce the conclusions from the previous section. Table 4 compares the experimental[4,88,89] $\beta_{\parallel}$ values for PNA in various solvents and at different wavelengths with data predicted by density functionals. Methods incorporating large amounts of exchange (HSE-HF, HISS-HF, and LC-ωPBE) provide good agreement with experiment in the gas phase but underestimate $\beta_{\parallel}$ in solution, i.e., have negative mean errors (ME). Tuning ω for each solvent reduces the mean absolute errors (MAEs) of HSE-HF and LC-ωPBE by about 10%. For HSE-HF*, the optimal ω values are 0.2, 0.4, and 0.4 au in 1,4-dioxane, acetone, and methanol, respectively; conversely, the optimal ω values in LC-ωPBE* decrease with increasing polarity.[55] That is, inclusion of larger portions of local exchange leads to better results in polar media. Indeed, in solution, HISS provides lower errors than HISS-HF, B3LYP yields rather good agreement with experiment, and HSE is similar to B3LYP. These observations suggest that cancellation occurs between the errors introduced by PCM and local exchange on the hyperpolarizabilities.

The dependence of the error in $\beta_{\parallel}$ on solvent and frequency is analyzed in Figure 4 and Table 5. All functionals have error

dx.doi.org/10.1021/jp510062b | J. Phys. Chem. A 2014, 118, 11787−11796

Table 5. Differences in Averages of Errors (ME/MAE in Percentage with Respect to Experiment) in $\beta_{\parallel}$ at 1064 nm and Infinite Wavelength (Static Limit), and in Different Media for PNA Calculated Using Data from Table 4

difference	HSE-HF	LC-ωPBE	LC-ωPBE*	HISS	HISS-HF	HSE-HF*	HSE	B3LYP
1064 nm−inf[a]	−11/11	−10/10	13/7	−7/7	−11/11	−13/13	−1/7	2/7
dioxane−gas[b]	−22/22	−28/25	25/25	−33/33	−28/15	−22/22	−35/−35	−37/−37
acetone−gas[b]	−33/33	−45/41	−11/−11	−57/−16	−45/33	−16/16	−64/−42	−68/−58
MeOH−gas[b]	−43/−43	−56/53	−25/−3	−73/0	−58/45	−31/31	−82/−24	−87/−38
acetone−dioxane[c]	5/−5	1/−1	−3/−21	1/−2	2/−2	23/−23	0/−10	0/−13
MeOH−acetone[c]	−11/11	−12/12	−14/2	−16/13	−12/12	−14/14	−17/9	−18/5
MeOH−dioxane[c]	−6/6	−10/10	−16/−23	−14/11	−10/10	−9/9	−17/−1	−18/−8

[a]Using all data at 1064 nm and infinite wavelength in solution. [b]Using data at 1064 nm only (to avoid bias from the dependence of the error on the frequency). [c]Using data at 1064 nm and infinite wavelength.

dependency on the wavelength; the MAE increases by about 10% when going from the static limit (infinite wavelength) to 1064 nm (Figure 4, top right panel). Likewise, the error also depends strongly on the solvent (Figure 4, bottom panels) with most functionals having rather similar dependencies except (to a certain extent) for the tuned LC-ωPBE* and HSE-HF*. These two methods include different fractions of HF exchange in different solvents, again emphasizing that the exchange energy (be it short or long range) is of critical importance to describe hyperpolarizabilities,[21,22,35] and their dependence on the media.[55,89] Additionally, the largest dependencies on the error are seen for the solvent/gas averages of differences in Table 5. The solvent cavity structure around the target molecule may thus be important to describe hyperpolarizabilities in solution; evidence for this has been found before too.[90,91] In fact, in ref 55 we concluded that PCM-TDDFT was insufficient to describe the dependence of $\beta_{\parallel}$ on solvent and frequency, at least for GGAs, global hybrids, and LC-DFT (although tuning ameliorates the issue). Here, we see that this statement extends to SR and MR hybrids, which display the same trends as functionals evaluated in ref 55.

Before closing this section, we should remark that there are inaccuracies in the theory−experiment comparisons just discussed. In particular, the DFT calculations neglect vibrational contributions to $\beta_{\parallel}$, and experimental data are expected to have a certain margin of error. However, the magnitude of these errors is unlikely to affect the general trends noted above. Although vibrational contributions to hyperpolarizabilities can be important in some cases, the vibrational contributions to $\beta_{\parallel}$ in PNA have been estimated to reduce the hyperpolarizability by no more than about 5% at the frequencies considered here.[89,92] Likewise, the error in the gas-phase measurement of $\beta_{\parallel}$ is reported to be 4%.[85] Furthermore, in ref 55 the methods providing best agreement with the experimental data in Table 4 were also found to agree the most with MP2 hyperpolarizabilities, which can be expected to be reasonably accurate.[42,70,73,89] Hence, recapitulating, SR and MR hybrids can give results similar to those of global hybrids and LC-DFT, all functionals have poor solvent and frequency dependencies, and these observations are likely to hold in spite of the possible inaccuracies in our theory−experiment comparisons.

2,3-DIHYDRO-1*H*-INDEN-1-ONE DERIVATIVES

Here, we evaluate the first-order NLO properties of the 2,3-dihydro-1*H*-inden-1-one derivatives **1**−**4** by applying the DFT methods discussed in the previous sections and MP2 calculations. The purpose of this section is 3-fold: (1) assess the potential NLO capabilities of **1**−**4**, (2) evaluate the effect of the different rings attached to the 2,3-dihydro-1*H*-inden-1-one ring on the hyperpolarizability, and (3) reinforce the results of the previous sections by analyzing chromophores that differ from the more ideal PNA and DANS*n*.

Table 6 lists the static β_{tot} values calculated by different methods for **1**−**4**. All methods agree in that the hyperpolarizabilities of **1** and **2** are rather similar and considerably lower than those of **3** and **4**, which are in turn close to each other. However, the exact values differ significantly between methods. The smallest hyperpolarizabilities are given by HF, whereas the largest are by B3LYP. This sort of underestimation/overestimation pattern is normally expected for CT compounds and, according to the diagnostic tool proposed in ref 55, we can expect LC-DFT methods to provide reasonable β_{tot} estimates. Considering that MP2 usually yields reasonable, albeit somewhat overestimated, hyperpolarizability values,[42,70,73,89] it would appear that B3LYP and HSE are overestimating β_{tot} whereas HF, LC-ωPBE, HSE-HF, and M06-HF are underestimating it. The rest of the methods lay between these extremes; LC-ωPBE* (which uses ω = 0.2 au for all four chromophores) is, in general, in good agreement with MP2. Once more, the long-range exchange does not appear to be of special importance to determine β_{tot}; HSE is similar to B3LYP; HSE-HF to M06-HF and LC-ωPBE; and HISS-HF to ωB97X-D and CAM-B3LYP.

Table 6. Static β_{tot} Values (au) Calculated by Different Methods for 1−4[a]

method	1	2	3	4
MP2	2416	2349	3534	3977
HF	1281	1068	1745	1880
B3LYP	2553	3432	4975	4942
HSE	2549	3355	4793	4783
CAM-B3LYP	2031	2179	3312	3502
ωB97X-D	1964	2025	3123	3269
LC-ωPBE	1691	1620	2607	2848
LC-ωPBE*	2166	2844	3737	3861
HISS	2381	2829	4096	4191
HISS-HF	1965	1997	2936	3117
HSE-HF	1463	1262	1883	2340
M06-HF	1670	1514	2302	2640

[a]MP2 uses the 6-31+G(d) basis; HF and DFT, the 6-31+G(d,p) basis. All geometries are CAM-B3LYP/6-31+G(d,p).

The calculations also indicate that **1**−**4** are all long-range CT compounds. In all cases, β_{tot} is dominated by a single component in the direction of the molecular dipole moment. In addition, **1**−**4** display substantial charge transfer in their excited states. This is illustrated in Figure 5, which shows the

dx.doi.org/10.1021/jp510062b | J. Phys. Chem. A 2014, 118, 11787−11796

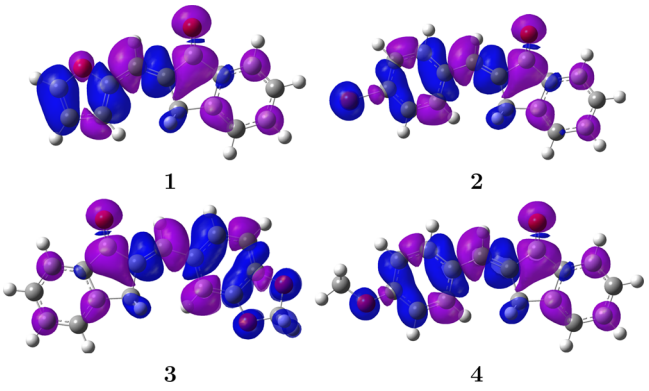

Figure 5. Difference in total electronic density (isocontour value of 4×10^{-4} au) between the ground and CT excited states of **1**−**4** at the LC-ωPBE/6-311+G(d,p) level. Purple (blue) regions indicate a gain (loss) of density in the excited state.

difference in total electronic density between the ground and CT excited states of **1**−**4** at the LC-ωPBE/6-311+G(d,p) level; other methods yield similar-looking density plots. These figures reveal considerable delocalization of the transferred charge across the ring in which the donor group is attached; the charge gained in the excited state is more localized on the CO group of the 2,3-dihydro-1H-inden-1-one. Note how in **2** and **4** the methoxy and Br groups, respectively, along with the carbons oriented *ortho* and *para* to these groups, act as donors, whereas *meta* carbons behave like acceptors. This reflects the well-known *ortho*/*para* director abilities of the methoxy and Br group in electrophilic aromatic substitutions. The methoxy group is a stronger donor and has its charge more localized than the Br group, which is presumably the main reason for the increase of about 80% in β_{tot} when going from **2** to **4** (because their structures differ only by these groups). Likewise, the furan ring of **1** can be expected to be a weaker donor than the 1,3-benzodioxol of **3**, and the β_{tot} of the latter is approximately 50% higher than that of the former. Thus, the calculations here not only agree with what could be expected from chemical intuition but also furnish the qualitative predictions of the latter with quantitative data that can be expected to be reasonably accurate.

CONCLUSIONS

We have demonstrated that, opposite to common belief, the long-range exchange potential is not of particular importance in the description of hyperpolarizabilities of prototypical long-range CT compounds. Instead, incorporation of substantial fractions of HF exchange across large portions of the molecule, which reduces the self-interaction error, appears to be the reason behind the relative success of various range-separated hybrids. Nevertheless, when hyperpolarizabilities in polar media are calculated with approximate solvation models like PCM, other factors such as error cancellation may come into play too. In the gas phase, HSE-HF and HISS-HF, as well as LC-DFT and tuned LC-DFT, provide relatively good results when compared to experimental data and MP2 calculations for PNA; HISS, HSE, global hybrids, and tuned LC-DFT are better in solution (with nonequilibrium PCM). However, all of these methods have a poor dependence of the $\beta_{\|}$ error (with respect to experiment) on solvent and frequency, at least when using PCM-TDDFT to model these effects, although tuning ameliorates these issues to a certain degree. Still, the results here suggest that, with some minor modifications, available SR and MR functionals may be competitive with LC-DFT and tuned LC-DFT methods for hyperpolarizability predictions, which are the best DFT methods currently at hand for this type of calculations. Finally, we point out that our conclusions seem robust within the limits of the present study, given by sample size, the use of DFT geometries, and the comparison to MP2 polarizabilities. All of these can be expected to be reasonably accurate.[24,26,42,46,70,73] We hope that this work will stimulate more extensive studies on the adequacy of SR and MR hybrids for the prediction of NLO properties of organic materials.

AUTHOR INFORMATION

Corresponding Author

*E-mail: guscus@rice.edu.

Notes

The authors declare no competing financial interest.

ACKNOWLEDGMENTS

The work at Rice University was supported by the US National Science Foundation (CHE-1110884). G.E.S. is a Welch Foundation Chair (C-0036).

REFERENCES

(1) Dreuw, A.; Weisman, J. L.; Head-Gordon, M. Long-Range Charge-Transfer Excited States in Time-Dependent Density Functional Theory Require Non-Local Exchange. *J. Chem. Phys.* **2003**, *119*, 2943−2946.

(2) Autschbach, J. Charge-Transfer Excitations and Time-Dependent Density Functional Theory: Problems and Some Proposed Solutions. *ChemPhysChem* **2009**, *10*, 1757−1760.

(3) Oudar, J. L.; Chemla, D. S. Hyperpolarizabilities of the Nitroanilines and Their Relations to the Excited State Dipole Moment. *J. Chem. Phys.* **1977**, *66*, 2664−2668.

(4) Reis, H. Problems in the Comparison of Theoretical and Experimental Hyperpolarizabilities Revisited. *J. Chem. Phys.* **2006**, *125*, 014506(1−9).

(5) Champagne, B.; Kirtman, B. Evaluation of Alternative Sum-Over-States Expressions for the First Hyperpolarizability of Push-Pull π-Conjugated Systems. *J. Chem. Phys.* **2006**, *125*, 024101(1−7).

(6) Garza, A. J.; Osman, O. I.; Wazzan, N. A.; Khan, S. B.; Asiri, A. M.; Scuseria, G. E. A Computational Study of the Nonlinear Optical Properties of Carbazole Derivatives: Theory Refines Experiment. *Theor. Chem. Acc.* **2014**, *133*, 1458(1−8).

(7) Garza, A. J.; Osman, O. I.; Wazzan, N. A.; Khan, S. B.; Asiri, A. M.; Scuseria, G. E. Prediction of the Linear and Nonlinear Optical Properties of Tetrahydronaphthalone Derivatives Via Long-Range Corrected Hybrid Functionals. *Mol. Phys.* **2014**, DOI: 10.1080/00268976.2014.934312.

(8) Hurst, M.; Munn, R. W. In *Organic Materials for Nonlinear Optics*; Hann, R. A., Bloor, D., Eds.; The Royal Society of Chemistry: London, 1989.

(9) Kanis, D. R.; Ratner, M. A.; Marks, T. J. Design and Construction of Molecular Assemblies with Large Second-Order Optical Nonlinearities. Quantum Chemical Aspect. *Chem. Rev.* **1994**, *94*, 195−242.

(10) Ramakrishna, G.; Goodson, T., III. Excited-State Deactivation of Branched Two-Photon Absorbing Chromophores: A Femtosecond Transient Absorption Investigation. *J. Phys. Chem. A* **2007**, *111*, 993−1000.

(11) Chakrabarti, S.; Ruud, K. Large Two-Photon Absorption Cross Section: Molecular Tweezer as a New Promising Class of Compounds for Nonlinear Optics. *Phys. Chem. Chem. Phys.* **2009**, *11*, 2592−2596.

(12) Marder, S. R.; Sohn, J. E.; Stucky, G. D. *Materials for Non-Linear Optics: Chemical Perspectives*; ACS Symposium Series 45; American Chemical Society: Washington, DC, 1991.

(13) Boyd, R. W. *Nonlinear Optics*; Academic Press: New York, 1992.

(14) Marder, S. R. Organic Nonlinear Optical Materials: Where We Have Been and Where We Are Going. *Chem. Commun.* **2006**, *2*, 131−134.
(15) Irie, M. Diarylethenes for Memories and Switches. *Chem. Rev.* **2000**, *100*, 1685−1716.
(16) Kawata, S.; Kawata, Y. Three-Dimensional Optical Data Storage Using Photochromic Materials. *Chem. Rev.* **2000**, *100*, 1777−1788.
(17) Tian, H.; Yang, S. Recent Progresses on Diarylethene Based Photochromic Switches. *Chem. Soc. Rev.* **2004**, *33*, 85−97.
(18) Dvornikov, A. S.; Walker, E. P.; Rentzepis, P. M. Two-Photon Three-Dimensional Optical Storage Memory. *J. Phys. Chem. A* **2009**, *113*, 13633−13644.
(19) Kurtz, H.; Dudis, D. Quantum Mechanical Methods for Predicting Nonlinear Optical Properties. *Rev. Comput. Chem.* **1998**, *12*, 241−279.
(20) Sim, F.; Chin, S.; Dupuis, M.; Rice, J. E. Electron Correlation Effects in Hyperpolarizabilities of p-Nitroaniline. *J. Phys. Chem.* **1993**, *97*, 1158−1163.
(21) Bulat, F. A.; Toro-Labbé, A.; Champagne, B.; Kirtman, B.; Yang, W. Density-Functional Theory (Hyper)polarizabilities of Push-Pull π-Conjugated Systems: Treatment of Exact Exchange and Role of Correlation. *J. Chem. Phys.* **2005**, *123*, 014319(1−7).
(22) Bokhan, D.; Bartlett, R. J. Exact-Exchange Density Functional Theory for Hyperpolarizabilities. *J. Chem. Phys.* **2007**, *127*, 174102(1−9).
(23) Champagne, B.; Perpète, E. A.; van Gisbergen, S. J. A.; Baerends, E. J.; Snijders, J. G.; Soubra-Ghaoui, C.; Robins, K. A.; Kirtman, B. Assessment of Conventional Density Functional Schemes for Computing the Polarizabilities and Hyperpolarizabilities of Conjugated Oligomers: An ab Initio Investigation of Polyacetylene Chains. *J. Chem. Phys.* **1998**, *109*, 10489−10498.
(24) Champagne, B.; Perpète, E. A.; Jacquemin, D.; van Gisbergen, S. J. A.; Baerends, E. J.; Soubra-Ghaoui, C.; Robins, K. A.; Kirtman, B. Assessment of Conventional Density Functional Schemes for Computing the Dipole Moment and (Hyper)polarizabilities of Push-Pull π-Conjugated Systems. *J. Phys. Chem. A* **2000**, *104*, 4755−4763.
(25) Loboda, O.; Zaleśny, R.; Avramopoulos, A.; Luis, J. M.; Kirtman, B.; Tagmatarchis, N.; Reis, H.; Papadopoulos, M. G. Linear and Nonlinear Optical Properties of [60]Fullerene Derivatives. *J. Phys. Chem. A* **2009**, *113*, 1159−1170.
(26) Garza, A. J.; Osman, O. I.; Scuseria, G. E.; Wazzan, N. A.; Khan, S. B.; Asiri, A. M. Nonlinear Optical Properties of DPO and DMPO: A Theoretical and Computational Study. *Theor. Chem. Acc.* **2013**, *132*, 1384(1−7).
(27) Garza, A. J.; Osman, O. I.; Wazzan, N. A.; Khan, S. B.; Scuseria, G. E.; Asiri, A. M. Photochromic and Nonlinear Optical Properties of Fulgides: A Density Functional Theory Study. *Comput. Theor. Chem.* **2013**, *1022*, 82−85.
(28) Chen, K. J.; Laurent, A. D.; Jacquemin, D. Strategies for Designing Diarylethenes as Efficient Nonlinear Optical Switches. *J. Phys. Chem. C* **2014**, *118*, 4334−4345.
(29) Savin, A.; Flad, H. Density Functionals for the Yukawa Electron-Electron Interaction. *Int. J. Quantum Chem.* **1995**, *56*, 327−332.
(30) Iikura, H.; Tsuneda, T.; Yanai, T.; Hirao, K. A Long-Range Correction Scheme for Generalized-Gradient-Approximation Exchange Functionals. *J. Chem. Phys.* **2001**, *115*, 3540−3544.
(31) Yanai, T.; Tew, D. P.; Handy, N. C. A New Hybrid Exchange-Correlation Functional Using the Coulomb-Attenuating Method (CAM-B3LYP). *Chem. Phys. Lett.* **2004**, *393*, 51−57.
(32) Vydrov, O. A.; Heyd, J.; Krukau, A. V.; Scuseria, G. E. Importance of Short-Range Versus Long-Range Hartree-Fock Exchange for the Performance of Hybrid Density Functionals. *J. Chem. Phys.* **2006**, *125*, 074106(1−9).
(33) Vydrov, O. A.; Scuseria, G. E. Assessment of a Long-Range Corrected Hybrid Functional. *J. Chem. Phys.* **2006**, *125*, 234109(1−9).
(34) Jacquemin, D.; Perpète, E. A.; Vydrov, O. A.; Scuseria, G. E.; Adamo, C. Assessment of Long-Range Corrected Functionals Performance for $n \rightarrow \pi^*$ Transitions in Organic Dyes. *J. Chem. Phys.* **2007**, *127*, 094102(1−6).
(35) Tawada, Y.; Tsuneda, T.; Yanagisawa, S.; Yanai, T.; Hirao, K. A Long-Range-Corrected Time-Dependent Density Functional Theory. *J. Chem. Phys.* **2004**, *120*, 8425−8433.
(36) Kamiya, M.; Sekino, H.; Tsuneda, T.; Hirao, K. Nonlinear Optical Property Calculations by the Long-Range-Corrected Coupled-Perturbed Kohn−Sham Method. *J. Chem. Phys.* **2005**, *122*, 234111(1−10).
(37) Jacquemin, D.; Perpète, E. A.; Scuseria, G. E.; Ciofini, I.; Adamo, C. TD-DFT Performance for the Visible Absorption Spectra of Organic Dyes: Conventional versus Long-Range Hybrids. *J. Chem. Theory Comput.* **2008**, *4*, 123−135.
(38) Perpète, E. A.; Jacquemin, D.; Adamo, C.; Scuseria, G. E. Revisiting the Nonlinear Optical Properties of Polybutatriene and Polydiacetylene with Density Functional Theory. *Chem. Phys. Lett.* **2008**, *456*, 101−104.
(39) Jacquemin, D.; Perpète, E. A.; Scuseria, G. E.; Ciofini, I.; Adamo, C. Extensive TD-DFT Investigation of the First Electronic Transition in Substituted Azobenzenes. *Chem. Phys. Lett.* **2008**, *465*, 226−229.
(40) Song, J.; Watson, M. A.; Sekino, H.; Hirao, K. Nonlinear Optical Property Calculations of Polyynes with Long-Range Corrected Hybrid Exchange-Correlation Functionals. *J. Chem. Phys.* **2008**, *129*, 024117(1−8).
(41) Zaleśny, R.; Bulik, I. W.; Bartkowiak, W.; Luis, J. M.; Avramopoulos, A.; Papadopoulos, M. G.; Krawczyk, P. Electronic and Vibrational Contributions to First Hyperpolarizability of Donor-Acceptor-Substituted Azobenzene. *J. Chem. Phys.* **2010**, *133*, 244308(1−7).
(42) de Wergifosse, M.; Champagne, B. Electron Correlation Effects on the First Hyperpolarizability of Push-pull π-Conjugated Systems. *J. Chem. Phys.* **2011**, *134*, 074113(1−13).
(43) Jacquemin, D.; Perpète, E. A.; Medved, M.; Scalmani, G.; Frisch, M. J.; Kobayashi, R.; Adamo, C. First Hyperpolarizability of Polymethineimine with Long-Range Corrected Functionals. *J. Chem. Phys.* **2007**, *126*, 191108(1−4).
(44) Nguyen, K. A.; Rogers, J. E.; Slagle, J. E.; Day, P. N.; Kannan, R.; Tan, L.; Fleitz, P. A.; Pachter, R. Effects of Conjugation in Length and Dimension on Spectroscopic Properties of Fluorene-Based Chromophores from Experiment and Theory. *J. Phys. Chem. A* **2006**, *110*, 13172−13182.
(45) Zaleśny, R.; Bulik, I. W.; Mikołajczyk, M.; Bartkowiak, W.; Luis, J. M.; Kirtman, B.; Avramopoulos, A.; Papadopoulos, M. G. Critical Assessment of Density Functional Theory for Computing Vibrational (Hyper)polarizabilities. *AIP Conf. Proc.* **2012**, *1504*, 655−658.
(46) Garza, A. J.; Scuseria, G. E.; Khan, S. B.; Asiri, A. M. Assessment of Long-Range Corrected Functionals for the Prediction of Non-Linear Optical Properties of Organic Materials. *Chem. Phys. Lett.* **2013**, *575*, 122−125.
(47) Bulik, I. W.; Zaleśny, R.; Bartkowiak, W.; Luis, J. M.; Kirtman, B.; Scuseria, G. E.; Reis, H.; Avramopoulos, A.; Papadopoulos, M. G. Performance of Density Functional Theory in Computing Non-resonant Vibrational (Hyper)polarizabilities. *J. Comput. Chem.* **2013**, *34*, 1775−1784.
(48) Lu, S.-I. Assessment of the Global and Range-Separated Hybrids for Computing the Dynamic Second-Order Hyperpolarizability of Solution-Phase Organic Molecules. *Theor. Chem. Acc.* **2014**, *133*, 1439.
(49) Koopmans, T. Über die Zuordnung von Wellenfunktionen und Eigenwerten zu den einzelnen Elektronen eines Atoms. *Physica* **1934**, *1*, 104−113.
(50) Stein, T.; Kronik, L.; Baer, R. Reliable Prediction of Charge Transfer Excitations in Molecular Complexes Using Time-Dependent Density Functional Theory. *J. Am. Chem. Soc.* **2009**, *131*, 2818−2820.
(51) Stein, T.; Kronik, L.; Baer, R. Prediction of Charge-Transfer Excitations in Coumarin-Based Dyes Using a Range-Separated Functional Tuned From First Principles. *J. Chem. Phys.* **2009**, *131*, 244119(1−5).
(52) Stein, T.; Eisenberg, H.; Kronik, L.; Baer, R. Fundamental Gaps in Finite Systems from Eigenvalues of a Generalized Kohn−Sham Method. *Phys. Rev. Lett.* **2010**, *105*, 266802(1−4).

(53) Karolewski, A.; Stein, T.; Kümmel, S. Tailoring the Optical Gap in Light-Harvesting Molecules. *J. Chem. Phys.* **2011**, *134*, 151101(1−4).
(54) Sun, H.; Autschbach, J. Influence of the Delocalization Error and Applicability of Optimal Functional Tuning in Density Functional Calculations of Nonlinear Optical Properties of Organic Donor-Acceptor Chromophores. *ChemPhysChem* **2013**, *14*, 2450−2461.
(55) Garza, A. J.; Osman, O. I.; Asiri, A. M.; Scuseria, G. E. Can Gap Tuning Schemes of Long-Range Corrected Hybrid Functionals Improve the Description of Hyperpolarizabilities? *J. Phys. Chem. B* **2014**, DOI: 10.1021/jp507226v.
(56) Garrett, K.; Sosa Vazquez, X. A.; Egri, S. B.; Wilmer, J.; Johnson, L. E.; Robinson, B. H.; Isborn, C. M. Optimum Exchange for Calculation of Excitation Energies and Hyperpolarizabilities of Organic Electro-optic Chromophores. *J. Chem. Theory Comput.* **2014**, *10*, 3821−3831.
(57) Autschbach, J.; Srebro, M. Delocalization Error and "Functional Tuning" in Kohn−Sham Calculations of Molecular Properties. *Acc. Chem. Res.* **2014**, *47*, 2592−2602.
(58) Asiri, A. M.; Faidallah, H. M.; Al-Nemari, K. F.; Ng, S. W.; Tienkink, E. R. T. (2E)-2-(Furan-2-ylmethylidene)-2,3-dihydro-1H-inden-1-one. *Acta Crystallogr.* **2012**, *E68*, o1065.
(59) Asiri, A. M.; Faidallah, H. M.; Al-Nemari, K. F.; Ng, S. W.; Tienkink, E. R. T. (2E)-2-(40Bromobenzylidene)-2,3-dihydro-1H-inden-1-one. *Acta Crystallogr.* **2012**, *E68*, o755.
(60) Asiri, A. M.; Faidallah, H. M.; Al-Nemari, K. F.; Ng, S. W.; Tienkink, E. R. T. (2E)-2-[(2H-1,3-Benzodioxol-5-yl)methylidene]-2,3-dihydro-1H-inden-1-one. *Acta Crystallogr.* **2012**, *E68*, o1015.
(61) Asiri, A. M.; Faidallah, H. M.; Al-Nemari, K. F.; Ng, S. W.; Tienkink, E. R. T. (2E)-2-(4-Methoxybenzylidene)-2,3-dihydro-1H-inden-1-one. *Acta Crystallogr.* **2012**, *E68*, o915.
(62) Henderson, T. M.; Izmaylov, A. F.; Scalmani, G.; Scuseria, G. E. Can Short-Range Hybrids Describe Long-Range-Dependent Properties? *J. Chem. Phys.* **2009**, *131*, 044108(1−9).
(63) Tozer, D. J. Relationship between Long-Range Charge-Transfer Excitation Energy Error and Integer Discontinuity in Kohn−Sham Theory. *J. Chem. Phys.* **2003**, *119*, 12697−12699.
(64) Heyd, J.; Scuseria, G. E.; Ernzerhof, M. Hybrid Functionals Based on a Screened Coulomb Potential. *J. Chem. Phys.* **2003**, *118*, 8207−8215.
(65) Henderson, T. M.; Izmaylov, A. F.; Scuseria, G. E.; Savin, A. The Importance of Middle-Range Hartree−Fock-type Exchange for Hybrid Density Functionals. *J. Chem. Phys.* **2007**, *127*, 221103(1−4).
(66) Henderson, T. M.; Izmaylov, A. F.; Scuseria, G. E.; Savin, A. Assessment of a Middle-Range Hybrid Functional. *J. Chem. Theory Comput.* **2008**, *4*, 1254−1262.
(67) Perdew, J. P.; Parr, R. G.; Levy, M.; Balduz, J. L. Density-Functional Theory for Fractional Particle Number: Derivative Discontinuities of the Energy. *Phys. Rev. Lett.* **1982**, *49*, 1691−1694.
(68) Willets, A.; Rice, J. E.; Burland, D. M.; Shelton, D. Problems in the Comparison of Theoretical and Experimental Hyperpolarizabilities. *J. Chem. Phys.* **1992**, *97*, 7590−7599.
(69) Frisch, M. J.; Trucks, G. W.; Schlegel, H. B.; Scuseria, G. E.; Robb, M. A.; Cheeseman, J. R.; Scalmani, G.; Barone, V.; Mennucci, B.; Petersson, G. A.; et al. *Gaussian 09*, Revision A.02; Gaussian Inc.: Wallingford, CT, 2009.
(70) Suponitsky, K. Y.; Tafur, S.; Masunov, A. E. Applicability of Hybrid Density Functional Theory Methods to Calculation of Molecular Hyperpolarizability. *J. Chem. Phys.* **2008**, *129*, 044109(1−11).
(71) Tomasi, J.; Mennucci, B.; Cammi, R. Quantum Mechanical Continuum Solvation Models. *Chem. Rev.* **2005**, *105*, 2999−3094.
(72) Hammond, J. R.; Kowalski, K. Parallel Computation of Coupled-Cluster Hyperpolarizabilities. *J. Chem. Phys.* **2009**, *130*, 194108(1−11).
(73) de Wergifosse, M.; Wautelet, F.; Champagne, B.; Kishi, R.; Fukuda, K.; Matsui, H.; Nakano, M. Challenging Compounds for Calculating Hyperpolarizabilities: p-Quinodimethane Derivatives. *J. Phys. Chem. A* **2013**, *117*, 4709−4715.
(74) Vydrov, O. A.; Scuseria, G. E.; Perdew, J. P. Tests of Functionals for Systems with Fractional Electron Number. *J. Chem. Phys.* **2007**, *126*, 154109(1−9).
(75) Drew, A.; Head-Gordon, M. Failure of Time-Dependent Density Functional Theory for Long-Range Charge-Transfer Excited States: The Zincbacteriochlorin−Bacteriochlorin and Bacteriochlorophyll−Spheroidene Complexes. *J. Am. Chem. Soc.* **2004**, *126*, 4007−4016.
(76) Brown, P. Kinetic Studies in Mass Spectrometry−IX: Competing [M−NO2] and [M−NO] Reactions in Substituted Nitrobenzenes. Approximate Activation Energies from Ionization and Appearance Potentials. *Org. Mass Spectrom.* **1970**, *4* (Suppl.), 533−544.
(77) Chowdhurry, S.; Kishi, H.; Dillow, G. W.; Kebarle, P. Electron Affinities of Substituted Nitrobenzenes. *Can. J. Chem.* **1989**, *67*, 603−610.
(78) Kosenov, D.; Slipchenko, L. V. Solvent Effects on the Electronic Transitions of *p*-Nitroaniline: A QM/EFP Study. *J. Phys. Chem. A* **2011**, *115*, 392−401.
(79) Rösch, N.; Trickey, S. B. Comment on "Concerning the Applicability of Density Funtional Methods to Atomic and Molecular Negative Anions. *J. Chem. Phys.* **1997**, *106*, 8940−8941.
(80) Sai, N.; Barbara, P. F.; Leung, K. Hole Localization in Molecular Crystals from Hybrid Density Functional Theory. *Phys. Rev. Lett.* **2011**, *106*, 226403(1−4).
(81) Imamura, Y.; Kobayashi, R.; Nakai, H. Linearity Condition for Orbital Energies in Density Functional Theory (II): Application to Global Hybrid Functionals. *Chem. Phys. Lett.* **2011**, *513*, 130−135.
(82) Atalla, V.; Yoon, M.; Caruso, F.; Rinke, P.; Scheffler, M. Hybrid Density Functional Theory Meets Quasiparticle Calculations: A Consistent Electronic Structure Approach. *Phys. Rev. B* **2013**, *88*, 165122(1−8).
(83) Schmidt, T.; Kraisler, E.; Makmal, A.; Kronik, L.; Kümmel, S. A Self-Interaction-Free Local Hybrid Functional: Accurate Binding Energies vis-à-vis Accurate Ionization Potentials from Kohn-Sham Eigenvalues. *J. Chem. Phys.* **2014**, *140*, 18A510(1−14).
(84) Stäehlin, M.; Moylan, C. R.; Burland, D. M.; Willets, A.; Rice, J. E.; Shelton, D. P.; Donley, E. A. A Comparison of Calculated and Experimental Hyperpolarizabilities for Acetonitrile in Gas and Liquid Phases. *J. Chem. Phys.* **1993**, *98*, 5595−5603.
(85) Kaatz, P.; Donley, E. A.; Shelton, D. P. A Comparison of Molecular Hyperpolarizabilities From Gas and Liquid Phase Measurements. *J. Chem. Phys.* **1997**, *108*, 849−856.
(86) Teng, C. C.; Garito, A. F. Dispersion of the Nonlinear Second-order Optical Susceptibility of Organic Systems. *Phys. Rev. B* **1983**, *28*, 6766−6773.
(87) Cheng, L.-T.; Tam, W.; Stevenson, S. H.; Meredith, G. R.; Rikken, G.; Marder, S. R. Experimental Investigations of Organic Molecular Nonlinear Optical Polarizabilities. 1. Methods and Results on Benzene and Stilbene Derivatives. *J. Phys. Chem.* **1991**, *95*, 10631−10643.
(88) Cheng, L.-T.; Tam, W.; Stevenson, S. H.; Meredith, G. R.; Rikken, G.; Marder, S. R. Experimental Investigations of Organic Molecular Nonlinear Optical Polarizabilities. 2. A Study of Conjugation Dependences. *J. Phys. Chem.* **1991**, *95*, 10643−1052.
(89) Day, P. N.; Pachter, R.; Nguyen, K. A. Analysis of Nonlinear Optical Properties in Donor-Acceptor Materials. *J. Chem. Phys.* **2014**, *140*, 184308(1−13).
(90) Mikkelsen, K. V.; Luo, Y.; Ågren, H.; Jørgensen, P. Solvent Induced Polarizabilities and Hyperpolarizabilities of para-Nitroaniline Studied by Reaction Field Linear Response Theory. *J. Chem. Phys.* **1994**, *100*, 8240−8250.
(91) Jensen, L.; van Duijnen, P. T. The First Hyperpolarizability of p-Nitroaniline in 1,4-Dioxane: A Quantum Mechanical/Molecular Mechanics Study. *J. Chem. Phys.* **2005**, *123*, 074307(1−7).
(92) Quinet, O.; Champagne, B.; Kirtman, B. Zero-Point Vibrational Averaging Correction for Second Harmonic Generation in para-Nitroaniline. *J. Mol. Struct.: THEOCHEM* **2003**, *633*, 199−207.